ISSN(Online) : 2319 -8753
ISSN (Print) : 2347 -6710

International Journal of Innovative Research in Science, Engineering and Technology

(An ISO 3297: 2007 Certified Organization)

Vol. 4, Issue 10, October 2015

Simultaneous Iterative Reconstruction Technique by Selective Discrimination SIRT-DS

Ivan Basile Kabiena [1], Emmanuel Tonye [2]

PhD Student, Department of Electrical and Telecommunication Engineering, National Advanced School of Engineering, Yaoundé, Cameroon [1]

Professor, Department of Electrical and Telecommunication Engineering, National Advanced School of Engineering, Yaoundé, Cameroon [2]

ABSTRACT: Iterative tomographic reconstructions models provide a better measure of the error in the process with the consequent elimination of artifact in the solution image. Selective discrimination associated with the SIRT method (SIRT-DS) offers a significant improvement in comparison with literature feel. The projections are grouped into windows based on their statistical similarities before they are processed by the SIRT method. Convergence is established when the standard deviation becomes stable in the first majority of reconstructed windows.

KEYWORDS: Discrimination, Iteration, Reconstruction, Simultaneous, Tomography.

I. INTRODUCTION

The word tomography is divided into two parts: tomo and graphy. The tomo root comes from ancient Greek and means to cut. The graph root comes from the ancient Greek and Latin and means writing [1]. Tomography is therefore to reconstruct the volume of an object by cuts from external measures. Then, as the name suggests, PET (Positron Emission Tomography) based on positron emission. These are emitted by decay of radioactive isotopes specific, which give rise to the encounter of matter, the creation of two gamma photons (γ) diametrically opposed [2]. A detector ring is then used to detect these photons. For each pair of photons detected, it is known that their point of emission is situated on the line joining the two points of detection [3] (Fig.1).

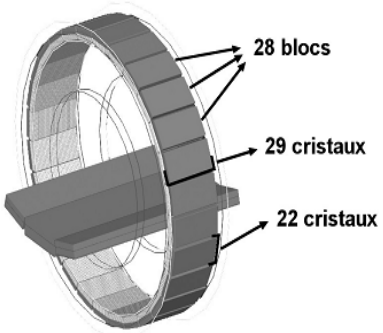

Fig.1. Complete Philips GEMINI GXL diagram composed of 28 blocks themselves composed of 22 × 29 crystals [4].

By measuring a number of pairs of photons, we will be able, via mathematical techniques, to obtain a picture considering the global distribution of emission locations of these photons [5]. PET is a functional imaging modality, that is to say it is used to characterize functional mechanisms in a living organism with a positron-emitting isotope. The most studied function is glucose metabolism. We injected to the patient (or animal) a glucose analogue labeled with the isotope ^{18}F, positon emitter. By detecting photon pairs and by finding

ISSN(Online) : 2319 -8753
ISSN (Print) : 2347 -6710

International Journal of Innovative Research in Science, Engineering and Technology

(An ISO 3297: 2007 Certified Organization)

Vol. 4, Issue 10, October 2015

their emission sites will be obtained after reconstruction of the signals, an image of the distribution of glucose in the body [6].

After this very brief situational, we now describe in detail all the steps to reach these tomographic images. After the detection and storage of photons in coincidence, another step is required to obtain a picture considering the distribution of the radiotracer in the organ or observed volume (FOV). This step is called tomographic reconstruction. It is performed using computers because whatever the method used, it requires a large number of operations [7]. To represent the distribution of radio-elements, it is common to be limited to a portion of the rectangular space right aligned with the cartesian axes.

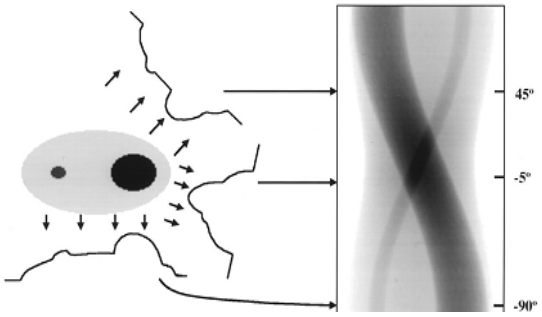

Fig.2. Example of sinogram (right) and its link with the projections in space (left). [4]

In 2D, it is a square whose size is equal to the side transaxial dimension FOV_t of FOV (fielf of view). In 3D, this portion of the space is extended along the axis of the detector and its dimension is equal to FOV_a (axial dimension FOV). This portion defined then the picture volume. Then it is discretized in small volume elements. In most cases, these elements are also parallelepipeds rights aligned cartesian axes. They are all identical and characterized by three dimensions representing the size of the sides along the axes X, Y and Z. In 2D, these elements are called pixels and voxels in 3D. Each pixel or voxel is set to the concentration of radionuclide contained therein. By definition, this value is positive or zero. This decomposition of the image into voxels is the most common but is not the only one. Historically, the first scanners operating in 2D, that is to say they only recorded coincidences involving two crystals of the same ring or of two adjacent rings. Reconstruction methods developed at this time were therefore adapted to reconstruct 2D [8]. Technology was then used to operate 3D scanners, thereby increasing the number of LORs (lines of response) or possible coincidences. There are analytical methods and iterative reconstructions according to the desired solution [9]. The work of S. Coolsa [8] and F. Lamare [9] that served as a basis of this paper, including their studies on the artifacts and noise are used to identify the different contributions of this research work.

II. TOMOGRAPHIC ITERATIVE RECONSTRUCTION METHODS

An iterative algorithm consists of a set of recovery operations and projections called iteration [10]. A reconstruction is the operator that provides a cutting from a sinogram (fig.2 and fig.3). Projection is the opposite operation, which calculates the sinogram for a particular cut.

During the iterative reconstruction, the iterations are repeated to obtain a theoretically nearest section of the solution as the previous cut. To achieve this, it is necessary to generate, during each iteration, an estimated sinogram. This is obtained by comparing the projection of the section obtained at the previous iteration and the measured sinogram [11].

ISSN(Online) : 2319 -8753
ISSN (Print) : 2347 -6710

International Journal of Innovative Research in Science, Engineering and Technology

(An ISO 3297: 2007 Certified Organization)

Vol. 4, Issue 10, October 2015

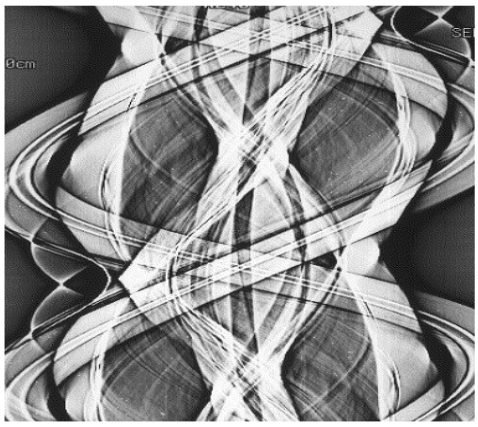

Fig.3. Example of sinogram [4]

The estimated sinogram is rebuilt by the next iteration to provide a new estimate of the cut. This cycle is repeated until the difference between the measured and estimated sinogram is smaller than the desired limit. We say that the algorithm has converged [12].

Iterative algorithms will be distinguished by the methods that are implemented to compare sinogram. The most commonly used PET algorithm is derived from the methods EM (Expectation Maximization) [13] accelerated by the principle of ordered subsets (ordered subset), which corresponds to the OSEM [14] symbol. Iterative reconstruction can eliminate artifacts in a star around the hyperfixantes structures (Fig 4). However, their implementation results in an increase in the calculation time. This is explained by the number of operations to be performed for each of the iterations. However, current informatics resources allow using these algorithms in clinical practice [15].

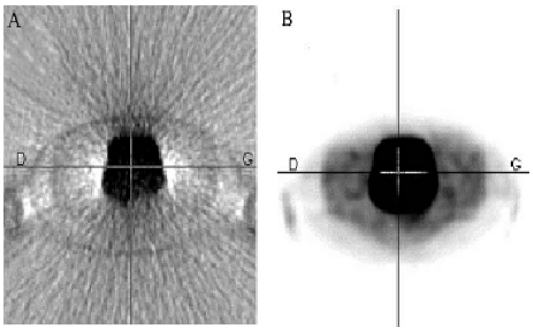

Fig.4. Two sections reconstructed by filtered back projection and iterative respectively at A and B

At this level there are the ART method (algebraic reconstruction method) faster, and SIRT method (simultaneous iterative reconstruction technology) more accurate but slower, hence the interest to improve [16] [17].

III. THE NEW APPROACH OF SIRT METHOD

III.1. THE SIRT METHOD

The method consist in the correction of f_i using all rays passing through x_i, as shown in Fig.5.
The equation to evaluate $f^{(k)}$ by correction $f^{(k-1)}$ is:

$$f_i^{(k)} = f_i^{(k-1)} + \frac{\sum_j p_j}{\sum_j \sum_i R_{ji}} - \frac{\sum_j R_j f^{(k-1)}}{\sum_j \|R_j\|^2} \quad (1)$$

ISSN(Online) : 2319 -8753
ISSN (Print) : 2347 -6710

International Journal of Innovative Research in Science, Engineering and Technology

(An ISO 3297: 2007 Certified Organization)

Vol. 4, Issue 10, October 2015

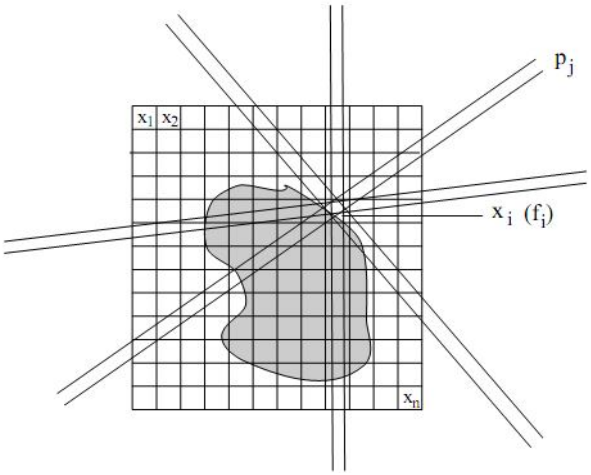

Fig.5. Principle of the SIRT method

This method provides a better quality of reconstructed slices.

III.2. SETS TO SUBSETS

Cantor is the main creator of set theory that he introduced in the early 1880 is working on problems of convergence of trigonometric series in the 1870, he has define a notion deriving sets of real numbers. The applications of his work has been extraordinarily influential and had numerous and various applications in mathematical logic and signal processing particularly in the context of this work.

P = {1, 2, 3, 4, 5} is a set consisting of five elements and there is ***card {P}*** = 5.

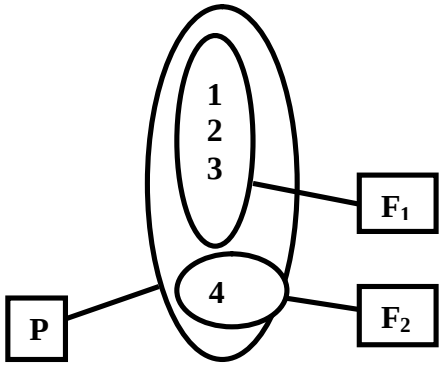

Diagram.1. Distribution of a set subassembly

Separating a whole into parts forming pieces of sets, subsets (see diagram 1). All elements of a wireless sub-set F_i of the set P belong to P.
By applying the consequences of this theory to projections from the tomograph, we deduce that there exists in the set P projections, subsets that can organize dimensions window M*N times according to their value (intensity of future pixels);
So if we consider P is four windows F_i as is the case in the context of this work, then

ISSN(Online) : 2319 -8753
ISSN (Print) : 2347 -6710

International Journal of Innovative Research in Science, Engineering and Technology

(An ISO 3297: 2007 Certified Organization)

Vol. 4, Issue 10, October 2015

$$Card\{P\} = \sum_{i=1}^{4} card\{F_i\} \quad (2)$$

The windows will therefore consist of close a value, which has the effect of increasing the inter-pixel correlation (see Fig 6). The noise is considered in this case as part of the image and rebuilt in the high frequencies, while the reverse operation, the effect of noise must therefore lessened justified by the triangle inequality explained as follows:

If

$$\|F_1\|^2 + \|F_2\|^2 \leq \|F_1 + F_2\|^2 \quad (3)$$

And

$$\|F_1\|^2 + \|F_2\|^2 < \|\mathbf{P}\|^2 \quad (4)$$

With ***E{X},*** the statistical error in the reconstruction by the SIRT method of a set or subset ***X***, Then,

$$cardE\{F_1\} + cardE\{F_2\} < cardE\{P\} \quad (5)$$

This inequality shows that the probability of introducing errors or parasites in treatment is reduced if we proceed with a piece by processing through a global treatment, so the necessity for a reconstruction by windows or sub-sets, with a quantifier effect on the error.

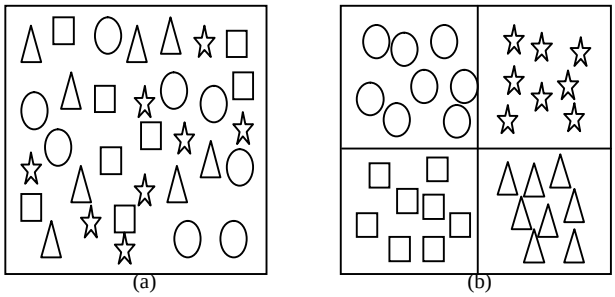

Fig.6.Set of non discriminate projection (a) subset of projection discriminated depending on the intensity with improvement in the correlation (b)

III.3. **SIRT-DS**

The SIRT-DS method stems from ART-DS approach differs from it on either the quality of the reconstructed image although slower compilation. The original image *I* is divided into four blocks of subsets and filled with zeros as described by the following summation:

$$I = \sum_{k=1}^{4} I_k + R_k(0) \quad (6)$$

This partitioning is proportional to the pixel of greatest intensity rating *M*. Combining equations (1) and (6) we obtain:

$$(I)_i^{(m)} = (I = \sum_{k=1}^{4} I_k + R_k(0))_i^{(m-1)} + \frac{\sum_j p_j}{\sum_j \sum_i R_{ji}} - \frac{\sum_j R_j (I = \sum_{k=1}^{4} I_k + R_k(0))^{(m-1)}}{\sum_j \|R_j\|^2} \quad (7)$$

This reflects an iterative block reconstruction following a discrimination proportional of M. The end of iterations or

ISSN(Online) : 2319 -8753
ISSN (Print) : 2347 -6710

International Journal of Innovative Research in Science, Engineering and Technology

(An ISO 3297: 2007 Certified Organization)

Vol. 4, Issue 10, October 2015

convergence of the algorithm is established when the value of the statistical variance becomes stable in the first majority of reconstructed blocks, so 3 over 4.

IV. EXPERIMENTS AND DISCUSSION

The results obtained have been done on a computer with two processors to reproduce as faithfully as the environment scanners available on the market. The basics of images are those phantoms Logan and Seismic representative sections of the brain and femur Fig.7 and Fig. 8 respectively.

Fig.7. Logan phantom showing a section of the brain

Fig.8. Seismic phantom representing a femoral cutting

After application of the selective discrimination at different numerical phantoms, we obtained in Fig.9 and Fig.10:

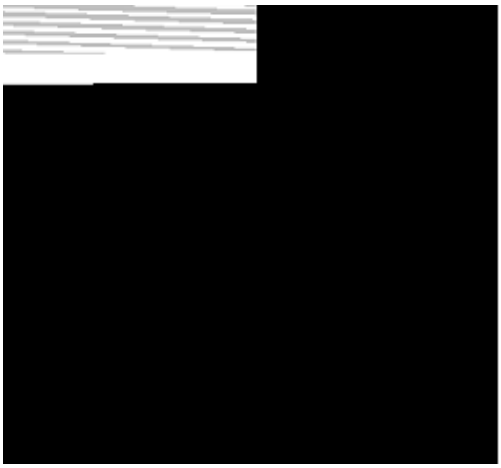

Fig.9. Selective discrimination of Seismic Phantom

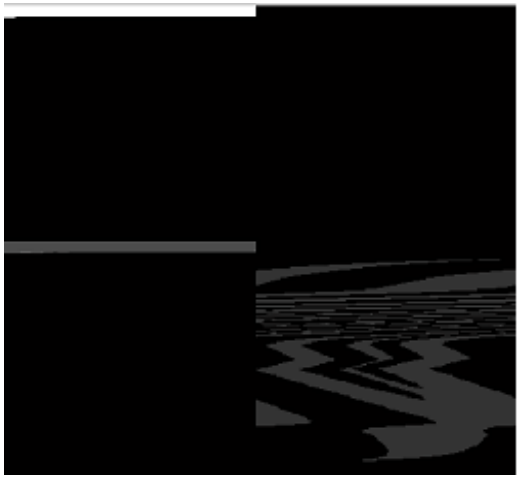

Fig.10. Selective discrimination of Logan phantom

Note that actually we are dealing with four blocks discriminated as theory predicts. For the seismic phantom, the main information of the original image is concentrated in the first dial which justifies the behavior of the curves in Fig.13 during the reconstruction. For the Logan phantom, the information is scattered throughout the blocks.

ISSN(Online) : 2319 -8753
ISSN (Print) : 2347 -6710

International Journal of Innovative Research in Science, Engineering and Technology

(An ISO 3297: 2007 Certified Organization)

Vol. 4, Issue 10, October 2015

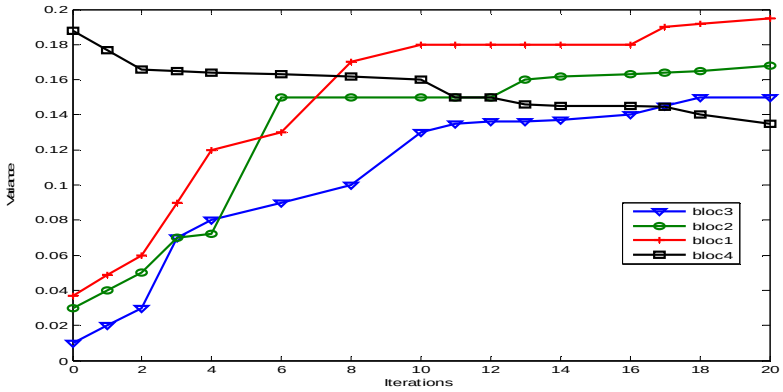

Fig.11. Evolution of the variance over the block iterations for the Logan phantom

By applying the method SIRT to these results with a 5% level of noise in the Logan phantom, it is noted that the algorithm converges after 10 iterations which results in a stability of the evolution of the variance for block 1 , block 2 and block 4 at iteration 10 (see Fig.11).

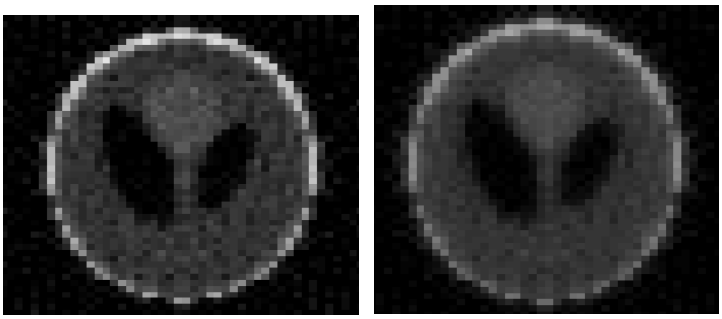

(a) (b)

Fig.12. Logan phantom rebuilt 2% (b) and 5% (c) of noise

Fig.12 shows the Logan rebuilt phantom by the SIRT-DS method after 7 iterations for a noise level of 2% and 10 iterations for a noise level of 5%. *The noise level increases the reconstruction time and the number of iterations.*

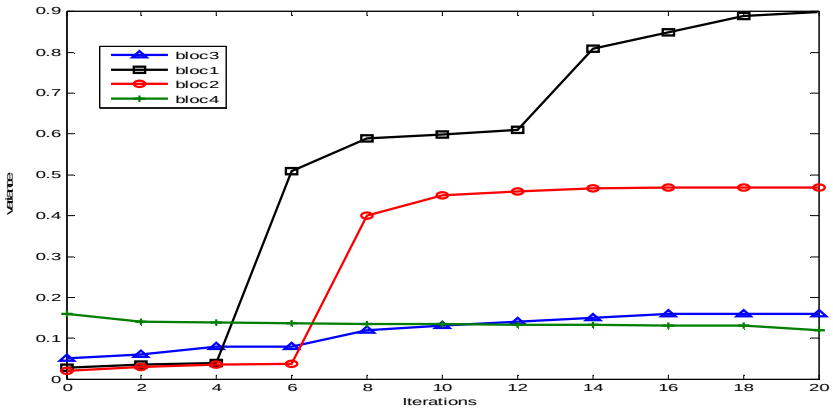

Fig.13. Evolution of the variance over the block iterations for the Seismic phantom

ISSN(Online) : 2319 -8753
ISSN (Print) : 2347 -6710

International Journal of Innovative Research in Science, Engineering and Technology

(An ISO 3297: 2007 Certified Organization)

Vol. 4, Issue 10, October 2015

Using the same experience this time with the seismic phantom, Fig.13 radiates a convergence after 6 iterations and 2% of noise. The constancy of the variance in block 1, block 2 and block 4 require stopping the iterations in this case also. For the two phantoms, block 3 diverges; specifically, this block has in both cases and specifically the majority of the noise introduced in the image during the reconstruction.

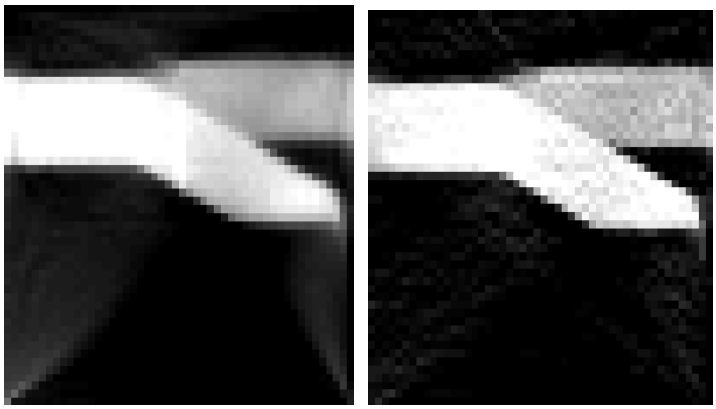

(b) (c)

Fig.14. Seismic phantom rebuilt with 2% (b) and 5% (c) of noise

Fig.14 shows the Seismic phantom rebuilt by the SIRT-DS method after 6 iterations to a noise level of 2% and 8 iterations to a noise level of 5%. Fig.14 (c) is visibly deteriorated as Fig.14 (b).

V. EVALUATION OF RESULTS

The table below provides a comparison of different approaches depending on the synthetic image used.

Table .1 Comparisons of results

Method	Phantom type	Noise level	Iteration	Reconstruction time
SIRT-DS	Logan	0.02	7	2.6s
ART-DS	Logan	0.02	8	2.9s
Kaczmarz	Logan	0.02	10	2.7s
Sym- Kaczmarz	Seismic	0.02	10	2.7s

The Study of the level of noise and iteration shows that the new approach set up offers a better rebuilt quality for greater reconstruction time. SIRT-DS method is faster at compile than other iterative methods studied here for the same base image types.

VI. CONCLUSION

The implementation of this new approach allows a wide range of choices according to the doctor that he favors the time or quality. However, the behavior of the third block requires further study to speculate discriminated filtering at the expense of the overall filtering generally applied in signal processing.

REFERENCES

[1] A. Alessio, C. Stearns, T. Shan et al,"Application and evaluation of a spatially varying Measured model system for PET image reconstruction" IEEE Trans. Med. Imaging, vol. 9, pp. 125-130, 2010

ISSN(Online) : 2319 -8753
ISSN (Print) : 2347 -6710

International Journal of Innovative Research in Science, Engineering and Technology

(An ISO 3297: 2007 Certified Organization)

Vol. 4, Issue 10, October 2015

[2] P. Arce, P. Rato, and J. Canadas Lagares "has GEANT4-based easy and flexible framework for nuclear medicine applications," IEEE Nucl. Sci. Symp. Conf. Rec. 2008

[3] S. Bacharach, M. Douglas, R. Carson, P. Kalkowski, et al, "Three-dimensional Registration of cardiac positron emission tomography scans attenuation", J. Nucl. Med., vol. 3, pp. 215-226, 1993

[4] F. Lamare, A. Turzo , Y. Bizais, et al. "Validation of a Monte Carlo simulation of the Philips Allegro / GEMINI PET systems using GATE", Phys. Med. Biol., vol. 51, pp.943–962, 2006

[5] D. Bailey, D. Townsend, P.Valk and M. Maisey, "Positron Emission Tomography", Springer Science Basis ,vol. 5, pp. 901-910, 2005

[6] H. Barrett and W. Swindell, "Radiological Imaging - The theory of imaging, detection, and processing" Ed Academic Press New York, Vol.50, pp. 4823–4840, 1981

[7] N. Belcari , F. Attanasi, S. Moehrs ,et al "A novel method for estimating random counts PET using asymmetrical delayed technical window and random single event acquisition" IEEE Nucl. Sci. Symp. Conf. Rec. pp.3611–3614, 2009

[8] S. Coolsa, P. Ghyselsb Wim van Aarlec, J. Sijbersc Wim Vanroose "A multi-level preconditioned Krylov method for the efficient solution of algebraic reconstruction tomography problems", Journal of Computational and Applied Mathematics, vol. 60, pp. 217-229, 2015

[9] S. Ben-Haim and P. Ell "18F-FDG PET and PET / CT in the assessment of cancer treatment response" J. Nucl. Med. Vol.50, pp. 88–99, 2009

[10] C. Cloquet, F. Elder, M. Defrise, et al, "Non-Gaussian space-varying resolution modeling for list mode reconstruction", Phys. Med. Biol. Vol.55, pp.5045–66, 2010

[11] M. Hatt, C. Rest Cheze , P. Dekker, et al "Accurate automatic delineation of heterogeneous functional positron emission tomography in volumes for oncology applications," Int. J. Radiat. Oncol. Biol. Phys. Vol. 77, pp. 301–308, 2010

[12] M. Lodge, A. Rahmim and R. Wahl, "Simultaneous measurement of noise and spatial resolution in PET phantom image", Phys. Med. Biol. Vol.55, pp.1069–1081, 2010

[13] K. Louis. "State of the Art and Future Development, Inverse Problems", Medical Imaging, 1992

[14] H. Alkadhi, T. Frauenfelder, D. Schmidt, "CT lung cancer screening - recent advance in radiology," Med Forum Switzerland. Vol.12, pp.25- 26, 2012

[15] B. Kelly Han, L. Grant, R. Garberich, "Assessment of an iterative reconstruction algorithm (SAFIRE) on image quality in pediatric cardiac CT datasets", Journal of Cardiovascular Computed Tomography, vol.6, pp. 200-204, 2012

[16] J. Floberg, F. Aaron Struck, K . Brooke, et al, "Impact of expectation-maximization reconstruction iterations on the diagnosis of temporal lobe epilepsy with PET," J Nucl Med Mol Am Imaging,vol. 2, n° 3,pp. 335-343, 2012

[17] P. Paleo and A. Mirone "Ring correcting artifacts in compressed sensing reconstruction tomography", Journal of Synchrotron Radiation, vol.3, pp.325-331, 2015